JOURNAL OF AIRCRAFT
Vol. 36, No. 2, March–April 1999

Suboptimal Damped Periodic Cruise Trajectories for Hypersonic Flight

Lael vonEggers Rudd* and Darryll J. Pines†
University of Maryland, College Park, Maryland 20742
and
Preston H. Carter II‡
Lawrence Livermore National Laboratory, Livermore, California 94550

An initial study of damped periodic flight trajectories that achieve optimal fuel savings for hypersonic flight is investigated. The aerodynamic characteristics of hypersonic lifting bodies including scramjet propulsion are used to achieve enhanced fuel savings compared with steady-state cruise. A parameterized form of the damped periodic altitude profile is assumed along with the constraint that the ratio of kinetic to potential energy remain the same at the endpoints of a period. Previous studies of periodic cruise neglected to impose this constraint, nor was a damped parameterized form of the altitude profile assumed. This resulted in suboptimal solutions of the two-point boundary-value problem for periodic hypersonic flight. This new parameterization along with the energy ratio constraint results in fuel savings of approximately 45% over the initial period for a modified model of the HL-20 spaceplane vehicle.

Nomenclature

A_e = engine inlet area
A_w = wing area
a = speed of sound
a_n, b_n = scalar Fourier series expansion constants
C_D = drag coefficient
C_{D0} = zero-lift drag coefficient
C_L = lift coefficient
$C_{L\alpha}$ = lift-curve slope
C_{L0} = zero angle-of-attack lift coefficient
$C_{T_{\max}}$ = maximum thrust coefficient
c = damping force constant
D = drag
F = force
h = absolute altitude
I_{sp} = specific impulse
J = cost function
k = spring force constant
L = lift
M = Mach number
m = mass
n = load factor
$\dot{Q}$ = heating rate
q = dynamic pressure
R_0 = Earth radius
r = range
r_d = end of forcing function
r_f = final range
r_u = start of forcing function
s = throttle
T = thrust
t = time
x = state position
$\dot{x}$ = state velocity
$\ddot{x}$ = state acceleration
α = angle of attack
β = momentum constant
γ = flight-path angle
ζ = damping ratio
η = exponential damping parameter
π = natural number
τ = dimensionless time
ϕ = phase angle
ω = $2\pi/r_f$
ω_d = damped natural frequency
ω_n = natural frequency

Subscripts
f = final
nc = nonconservative
nd = nondimensional
0 = initial

Received Sept. 1, 1997; revision received July 7, 1998; accepted for publication Aug. 4, 1998.

*Graduate Research Fellow, Department of Aerospace Engineering. Student Member AIAA.
†Assistant Professor, Department of Aerospace Engineering. Senior Member AIAA.
‡Research Engineer, Mechanical Engineering Division.

Introduction

IT has been proven that steady-state modes of engineering processes are not always optimal, and that cyclic, or periodic, control can produce greater efficiency. Prior to World War II, Sanger was the first known advocate of periodic control for aerospace vehicles to achieve long range for an intercontinental bomber. However, recent credit has been given to Edelbaum,[1] who in the 1950s analyzed the optimality of an energy-state model to show mechanisms for enhanced performance using periodic cruise.

State of the Art: Periodic Cruise

Twenty years following Edelbaum's study, a considerable amount of effort has been undertaken to determine optimal periodic trajectories for subsonic and hypersonic flight. Some of the more notable contributions in the study of periodic cruise are summarized in Table 1, which chronologically lists contributions to periodic cruise over the past 30 years. Although this table does not provide specific details regarding contributions made by the researchers listed, it does illustrate how a better understanding of periodic cruise trajectories has led to a steady improvement in fuel-consumption rate savings

Table 1 Contribution to periodic cruise research

Name	Year	Regime	Method	Optimization	Model	% fuel savings
Edelbaum[1]	1955	Subsonic	Th	Uncon	——	——
Zagalsky et al.[2]	1971	Subsonic	Th	Uncon	Generic	——
Schultz and Zagalsky[11]	1972	Subsonic	Th	Uncon	Various	——
Speyer[3]	1973	Subsonic	Th	Uncon	Generic	——
Schultz[12]	1974	Subsonic	Th	Uncon	Generic	——
Gilbert[4]	1976	Subsonic	Th	——	——	——
Gilbert and Parsons[13]	1976	Subsonic	Th/comp	Uncon	F-4/ideal	1.7
Speyer[5]	1976	Subsonic	Th/comp	Uncon	Generic	——
Houlihan et al.[6]	1982	Subsonic	Th/comp	Uncon	F-4E, RPV, Supercruiser	5.0
Speyer et al.[7]	1985	Hypersonic	Th/comp	Uncon	Generic	4.2
Grimm et al.[14]	1986	Subsonic	Comp	Con	F-4	2.0
Chuang and Speyer[8]	1987	Hypersonic	Th/comp	Uncon	Spaceplane	5.0
Sachs and Christodoulou[15]	1987	Subsonic	Th	Con	——	——
Speyer[16]	1996	——	——	——	——	Summary
Chuang and Morimoto[9]	1997	Hypersonic	Th/comp	Uncon/con	Spaceplane	8.1

Note: Th = theoretical work done, comp = computational work done, Con = optimization w/constraints, and Uncon = optimization without constraints.

compared with steady-state cruise. These steady improvements over time are primarily a result of three factors.

1) Theoretical advances in the optimality of periodic cruise (application of calculus of variations to necessary and sufficient conditions).

2) A better understanding of integrated vehicle flight dynamics for subsonic and hypersonic flight.

3) Improved optimization tools for solving unconstrained and constrained two-point boundary value problems (TPBVP).

Pioneering theoretical work in the study of periodic cruise was first performed by Zagalsky et al.,[2] and later by Speyer,[3] who proved that steady cruise was not a minimizing solution for minimum fuel consumption. Following this important result, Gilbert[4] was the first to demonstrate that time-dependent periodic control can improve the fuel economy of cruise vehicles. An F-4 vehicle model was shown to achieve a 1.7% fuel savings by flying along a periodic path.

As computational solutions began to validate earlier theoretical work, a better physical understanding of periodic cruise began to evolve from the application of theoretical results to various aircraft models. Speyer,[5] in his analysis of the nonoptimality of steady-state cruise, alludes to two reasons why cyclic control is better for improving the fuel consumption rate.

1) Fuel efficiency is improved at constant energy by *chattering* between states when the aircraft is aerodynamically efficient and power efficient with respect to thrust.

2) It is dynamic considerations that cause the nonoptimality of steady-state cruise.

A more detailed examination of chattering cruise was conducted by Houlihan et al.,[6] who attempted to relate the nonconvexity of periodic cruise to aerodynamic and propulsion parameters. Several subsonic aircraft models were considered and it was found that the best improvement in fuel savings that could be achieved was approximately 5%.

Application to Hypersonic Flight

The first application of periodic cruise to hypersonic vehicles was performed by Speyer et al.[7] In this work, second-order conditions for local optimality were applied to determine a closed, periodic path. The shooting method was used to solve the TPBVP. A solution for a flat Earth model was found to provide a local minimum, yielding a fuel savings of 4.2% over the steady-state cruise solution. This result suffered from poor atmosphere and vehicle models. More realistic aerodynamic and scramjet models for a hypersonic vehicle were later considered by Chuang and Speyer.[8] A minimizing boundary condition method was used to increase the region of convergence of the TPBVP. With engine-off drag penalties, little improvement over steady-state cruise was obtained. Without this penalty, however, fuel savings of 5% were realized.

Chuang and Morimoto[9] extended earlier work in periodic cruise to determine optimal periodic cruise trajectories for a hypersonic vehicle with constraints. These trajectories were determined using a suboptimal initial guess corresponding to a parameterized form of the altitude profile. This initial guess was then used in a minimization boundary condition optimization. Heating rates and load factors were used as constraints in the TPBVP optimization. The vehicle model was constructed using numerical data and design parameters from the HL-20 spaceplane. The unconstrained optimal solution showed an 8.12% fuel savings over steady-state cruise. With a heating rate constraint of 400 W/cm^2, the fuel savings reduced to 2.45%, which is close to the suboptimal solution. With a load factor constraint of 5 g, the fuel savings changed very little from the unconstrained solution. An optimal solution with both a heating-rate constraint of 1158 W/cm^2 and a load factor of 7 g produced a fuel savings of 8.09%.

Contribution of Current Work

Following the lead of previous researchers who have investigated optimal periodic cruise trajectories that achieve a minimal fuel-consumption rate, this work considers damped periodic cruise trajectories for hypersonic flight. The goal of this work is to find trajectories that minimize the fuel-consumption rate. However, in contrast to previous efforts, this work attempts to extend the concept of periodic optimal cruise to hypersonic trajectories that are damped by aerodynamic forces. A suboptimal solution to the TPBVP is computed, which does not force the initial and final state conditions of the trajectories to be equal. The final altitude, Mach number, and mass are allowed to be free with the constraint that the energy ratio of kinetic energy to potential energy (K.E./P.E.) over one cycle remain constant at the endpoints. A *bang-on–bang-off* solution is computed that corresponds to a local minimum for a parameterized form of the altitude profile.

In the next section, a spring-mass-damper system is presented as an analogous example of computing optimal trajectories for damped periodic hypersonic cruise. This example is developed to illustrate some of the fundamental concepts associated with damped periodic motion. Following this example, five parameterized altitude profiles are evaluated against a minimum fuel-consumption performance objective. An exponentially damped parameterized altitude profile is shown to achieve the best suboptimal solution.

Optimal Time-Averaged Damped Harmonic Motion

Forced Spring-Mass-Damper Analogy

Periodic flight trajectories can be considered to be analogous to the harmonic motion of the forced spring-mass-dashpot sys-

tem displayed in Fig. 1. Consider the equation of motion of a spring-mass-damper system given by

$$m\ddot{x} + c\dot{x} + kx = F \tag{1}$$

Dividing through by m, Eq. (1) can be written as

$$\ddot{x} + 2\zeta\omega_n\dot{x} + \omega_n^2 x = F/m \tag{2}$$

where the natural frequency is given by

$$\omega_n = \sqrt{k/m} \tag{3}$$

and ζ is given by

$$\zeta = c/2m\omega_n \tag{4}$$

For an underdamped response ($0 < \zeta < 1$) the free and forced solutions to this equation are given by the following equations.

Free:

$$x(t) = (A_1 e^{i\omega_d t} + A_2 e^{-i\omega_d t})e^{-\zeta\omega_n t} \tag{5}$$

or

$$x(t) = Ae^{-\zeta\omega_n t}\cos(\omega_d t - \phi) \tag{6}$$

Forced:

$$x(t) = \int_0^t \frac{1}{m} e^{-\zeta\omega_n\tau}\sin\omega_d\tau F(\tau)\,d\tau \tag{7}$$

where the damped natural frequency is given by

$$\omega_d = \omega_n\sqrt{1 - \zeta^2} \tag{8}$$

The total energy in the system is given by

$$E = \text{K.E.} + \text{P.E.} = \tfrac{1}{2}m\dot{x}^2 + \tfrac{1}{2}kx^2 \tag{9}$$

The rate of change of energy with respect to time caused by the viscous dissipation of energy in the damper and by the external load F is given by

$$\frac{dE}{dt} = m\dot{x}\ddot{x} + kx\dot{x} = -c\dot{x}\dot{x} + F\dot{x} = F_{nc}\dot{x} \tag{10}$$

which assumes that the mass remains constant. The subscript nc in Eq. (10) refers to all nonconservative forces acting on the system. By an appropriate choice of forcing, F, over a period of motion, the rate of energy loss, dE/dt, can be set equal to zero. This would imply that the initial and final state conditions over one period would remain the same. However, if $0 < F < c\dot{x}$, then the initial and final state conditions are not matched. Thus, the energy in the system must decrease as a result of dissipative forces.

If one were to compute the ratio of the K.E. to the P.E., this ratio would remain equal at the initial and final condition, whether the system was forced or not. This ratio can be computed from

$$\text{K.E./P.E.} = \tfrac{1}{2}m\dot{x}^2/\tfrac{1}{2}kx^2 \tag{11}$$

where the velocity for unforced motion is given by

$$\dot{x} = A(-\zeta\omega_n)e^{-\zeta\omega_n t}\cos(\omega_d t - \phi) + Ae^{-\zeta\omega_n t}[-\omega_d\sin(\omega_d t - \phi)] \tag{12}$$

Substituting the free vibration solution for x and $\dot{x}$ leads to

$$\frac{\text{K.E.}}{\text{P.E.}} = \frac{\tfrac{1}{2}m\{[\zeta\omega_n Ae^{-\zeta\omega_n t}\cos(\omega_d t - \phi) - \omega_d Ae^{-\zeta\omega_n t}\sin(\omega_d t - \phi)]\}^2}{\tfrac{1}{2}k[Ae^{-\zeta\omega_n t}\sin(\omega_d t - \phi)]^2} \tag{13}$$

At $t = 0$ and $2\pi/\omega_d$:

$$\frac{\text{K.E.}}{\text{P.E.}} = \frac{\tfrac{1}{2}m(\zeta\omega_n A\cos\phi + \omega dA\sin\phi)^2}{\tfrac{1}{2}k(-A\sin\phi)^2} \tag{14}$$

The energy ratio remains the same at the endpoints of a period. Similar results hold for the forced response solution of the spring-mass-damper system. However, in the forced system, a proportional term of the time of the force would be included. For the present work, it is assumed that the forcing time is small compared with the time of the period. This greatly simplifies the boundary condition relations.

Time-Averaged Objective Function

With this insight into periodic properties of the energy ratio, it is not difficult to formulate a fuel optimal cost function over one cycle that achieves minimum fuel expenditures, with the constraint that the energy ratio remain constant at the endpoints of a period. A cost function of time-averaged fuel consumption for the spring-mass-damper system takes the following form:

$$J = \frac{1}{t_f}\int_0^{t_f}\frac{F}{\dot{x} + 2}\,dt \tag{15}$$

where the constant term in the denominator of the expression in the integrand is used to avoid numerical difficulties when $\dot{x} = 0$. Nondimensionalizing the equation of motion for the spring-mass-damper permits the time-averaged cost to be represented as

$$J = \frac{1}{2\pi}\int_0^{2\pi}\frac{F_{nd}}{\dot{x}_{nd} + 2}\,d\tau \tag{16}$$

where the nondimensional time, position, and forcing arc are given by

$$\tau = \omega_d t \tag{17}$$

$$x_{nd} = x\omega_d^2/g \tag{18}$$

$$F_{nd} = F/mg = \beta(r_d - r_u)/mg \tag{19}$$

subject to

$$x(0) = \text{free}, \qquad \dot{x}(0) = \text{free} \tag{20}$$

$$x(2\pi) = \text{free}, \qquad \dot{x}(2\pi) = \text{free} \tag{21}$$

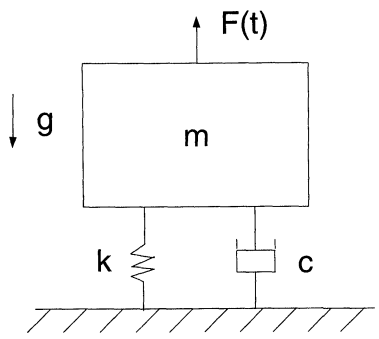

Fig. 1 Spring-mass-damper system.

and the constraint

$$\text{K.E./P.E.}(0) = (\text{K.E./P.E.})(2\pi) \tag{22}$$

Maintaining the constraint that the ratio of K.E./P.E. be held equal at the end conditions ($\tau = 0$ and 2π) permits the determination of an optimal solution. An example that attempts to minimize the cost in Eq. (16) using a bang-on–bang-off control force F, is presented in Fig. 2 for the hypothetical spring-mass-damper parameters listed in Table 2. The improvement in hypothetical fuel-consumption savings when compared with a damped periodic trajectory with the same initial and final conditions is significant. Table 2 shows that the cost for the damped trajectory is a factor of 20 less than that for the undamped solution. Also of interest is Fig. 3, which shows how the viscous force varies as a function of displacement x. It is easy to see that less effort is expended for the constant energy ratio TPBVP than for the case where the initial and final state conditions are equal. This suggests that damped periodic motion is more fuel-optimal than undamped periodic motion.

Insight from this spring-mass-damper example can be used to determine suboptimal periodic cruise trajectories for hypersonic flight. This is done in the next section by choosing a parameterized form of the altitude profile for unconstrained optimization. The source of damping in steady-state or periodic hypersonic cruise trajectories is a result of the nonlinear aerodynamic viscous forces acting on the hypersonic vehicle.

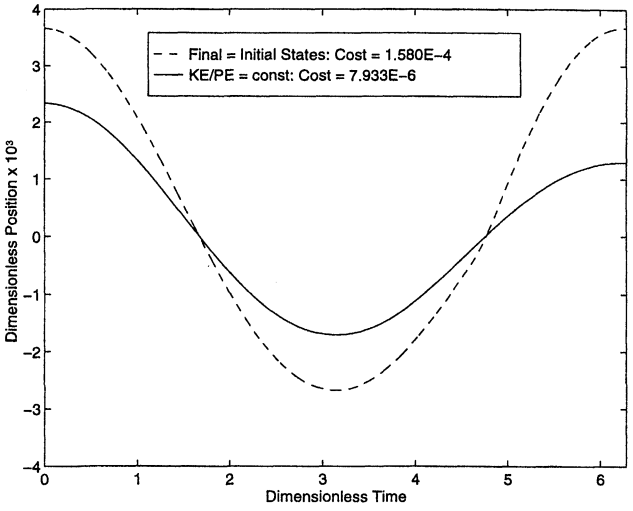

Fig. 2 Example of spring-mass-damper optimization.

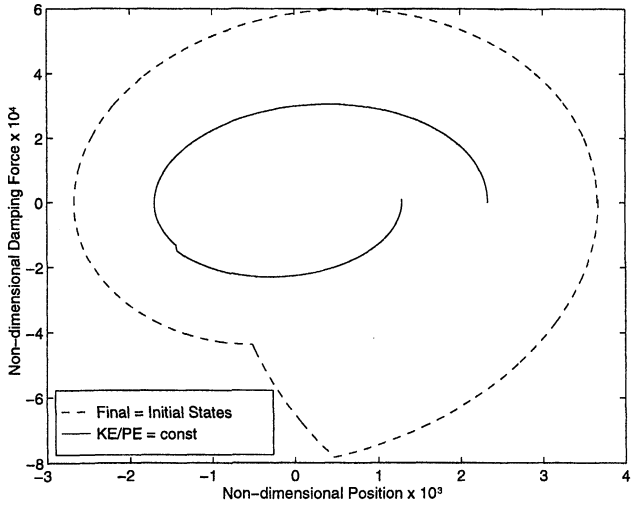

Fig. 3 Example of spring-mass-damper optimization.

Table 2 Nondimensional parameters for mass-spring-damper optimization example

Variable	$x(0) = x(2\pi)$	$x(0) \neq x(2\pi)$
$x_{\text{nd,initial}}$	3.657E-3	2.331E-3
$\dot{x}_{\text{nd,initial}}$	0.00	0.00
F_{nd}	6.626E-3	6.626E-3
τ_{on}	4.590 rad	3.711 rad
τ_{off}	4.890 rad	3.726 rad
τ_f	2π	2π
Cost	1.580E-4	7.933E-6

These forces act on the body in a way that is analogous to viscous damping of the spring-mass-damper system that was just presented. The effect of these forces can be approximated as imparting exponential damping to the amplitude of the trajectory. With this assumption, one can impose that the ratio of K.E. to P.E. is again equal at the endpoints of a period. This permits optimal ranged-average fuel-consumption rate trajectories to be determined, which are exponentially damped over a period of time. Properties of a modified HL-20 spaceplane vehicle, studied by Chuang and Morimoto,[9] are used here to provide comparative optimization results.

Suboptimal Periodic Cruise for Parameterized Altitude Profiles

Because hypersonic periodic flight trajectories appear to exhibit harmonic behavior, a parameterized form of the altitude profile consisting of only a few harmonics can come quite close to capturing the salient features of the unconstrained optimal trajectory. Because these harmonics are defined by constants, a suboptimal solution is possible by simply determining the parameters of the altitude profile. This results in less computational effort than a completely unconstrained optimization of the minimum fuel-consumption rate TPBVP.

Altitude Profile

The altitude profile for periodic flight can be approximated as a Fourier series expansion given by

$$h(r) = h_0 + \sum_{n=1}^{N} a_n \cos n\frac{2\pi}{r_f} r + \sum_{n=1}^{N} b_n \sin n\frac{2\pi}{r_f} r \qquad (n = 0, 1, 2, \ldots) \tag{23}$$

where the terms h_0, a_n, and b_n are scalars. In Chuang's and Morimoto's[9] work, a parameterization of altitude is used to obtain a good initial guess for a completely unconstrained optimization problem. The optimized solution to the parameterized problem is called a suboptimal solution. This work expands upon parameterized suboptimal minima found in that research, and shows that by an appropriate parameterization choice, better suboptimal solutions can be found that achieve greater fuel savings. Table 3 lists the various altitude profiles for each of the five parameterizations considered in this work.

Vehicle Dynamic Model

The equations of motion used herein are for flight in a vertical plane over a nonrotating spherical Earth, with range as an independent variable. The nonlinear equations of motion are given by

$$\frac{dh}{dr} = \tan\gamma\left(1 + \frac{h}{R_0}\right) \tag{24}$$

$$\frac{dM}{dr} = \frac{(T\cos\alpha - D - mg\sin\gamma)}{Ma^2 m\cos\gamma}\left(1 + \frac{h}{R_0}\right) \tag{25}$$

$$\frac{d\gamma}{dr} = \left(\frac{L + T\sin\alpha - mg\cos\gamma}{M^2a^2 m\cos\gamma} + \frac{1}{R_0 + h}\right)\left(1 + \frac{h}{R_0}\right) \tag{26}$$

Table 3 Parameterizations of altitude

Parameterization	Altitude profile	Conditions	State correlation
1	$h_a \cos(2\pi/r_f)r + h_b \cos(4\pi/r_f)r + h_c$	Speed-of-sound constant, mass constant, final range fixed	$x(0) = x(2\pi)$
2	$h_a \cos(2\pi/r_f)r + h_b \cos(4\pi/r_f)r + h_c$	Mass constant, final range fixed	$x(0) = x(2\pi)$
3	$h_a \cos(2\pi/r_f)r + h_b \cos(4\pi/r_f)r + h_c$	Final range fixed	$x(0) = x(2\pi)$
4	$h_a \cos(2\pi/r_f)r + h_b \cos(4\pi/r_f)r + h_c$	None	$x(0) = x(2\pi)$
5	$\exp[-\eta(r/r_f)][h_a \cos(2\pi/r_f)r + h_b \cos(4\pi/r_f)r] + h_c$	K.E./P.E. = constant at $(0, 2\pi)$	$x(0) \neq x(2\pi)$

$$\frac{dm}{dr} = -\frac{T}{gI_{sp}Ma\cos\gamma}\left(1 + \frac{h}{R_0}\right) \tag{27}$$

which correspond, respectively, to the change in height, Mach number, flight-path angle, and mass with respect to range.

The aerodynamic and engine models, developed by Chuang and Morimoto, use curve-fitted data taken from available the spaceplane literature.[9] The aerodynamic equations for drag and lift are given by

$$D = qC_DA_w \tag{28}$$

$$L = qC_LA_w \tag{29}$$

The drag and lift coefficients use a drag polar form given by

$$C_D = C_{D0}(M) + K(M)C_L^2 \tag{30}$$

$$C_L = C_{L0}(M) + C_{L\alpha}(M)\alpha \tag{31}$$

where

$$K(M) = 1.85[1 - \exp(-0.2356M)] \tag{32}$$

$$C_{L0}(M) = (1/20\pi)\arctan[10(M - 1)] - 0.035 \tag{33}$$

$$C_{L\alpha}(M) = 0.057\exp(-0.654M) + 0.014 \tag{34}$$

where $C_{D0} = 0.008$ (for Mach numbers above 6); $A_w = 250$ m^2; and $m_{\text{vehicle}} = 89{,}930$ kg.

The airbreathing engine model is described by

$$C_{T_{\max}}(M, \alpha) = \frac{15(\alpha + 5)0.25}{M^{1.15}}\exp\left\{-\frac{M^{0.08}}{200}[(\alpha + 5) - \frac{35}{M^{0.6}}]^2\right\} \tag{35}$$

$$T = sqC_{T_{\max}}A_e \tag{36}$$

where the throttle coefficient, s, lies in the range $0 \leq s \leq 1$, and the exit area of the engine is $A_e = 9.02$ m^2. It should be noted that, in this study, Mach 6 is the lowest speed that the vehicle is allowed to fly. A standard atmosphere was also used to get the values of the thermodynamic freestream variables. It was also assumed that the thrust would be of a bang-on–bang-off-type control.

An obvious concern for hypersonic vehicles flying these periodic trajectories is the g force loads and heating rates that will be incurred. For this study, the load factor, n, is calculated in number of g given by the following equation:

$$n = \frac{\sqrt{(T\cos\alpha - D)^2 + (L + T\sin\alpha)^2}}{mg} \tag{37}$$

The heating rate was estimated by Chuang and Morimoto,[9] for a stagnation point on a 10-cm radius nose cone using the equation:

$$\dot{Q} = 5.188 \times 10^{-8}\rho^{0.5}V^3 \tag{38}$$

Optimization

Cost Function

The function that is minimized is the range-averaged fuel-consumption rate. Mathematically, this function is expressed as

$$J = \frac{1}{r_f}\int_0^{r_f}\frac{T}{gI_{sp}Ma\cos\gamma}\left(1 + \frac{h}{R_0}\right)dr \tag{39}$$

This cost function is used for all cases, except for the steady-state constant mass problem. For this case, an instantaneous fuel-consumption rate is used:

$$J = \frac{T}{gI_{sp}Ma}\left(1 + \frac{h}{R_0}\right) \tag{40}$$

Optimizer

The parameter optimization is done with the design optimization tools (DOT) software package.[10] Because the optimizations of this work are constrained, the modified method of feasible directions algorithm of DOT is used. This algorithm attempts to 1) find a usable-feasible search direction, 2) find the scalar parameter that will minimize the cost subject to constraints, and 3) test for convergence. A more detailed explanation of this optimizer can be found in the DOT manual.[10]

Optimization Results for Parameterized Altitude Profiles

Parameterization 1

The first periodic altitude parameterization considered in this study is identical to the parameterization developed by Chuang and Morimoto,[9] and it is given by

$$h = h_a\cos\omega r + h_b\cos 2\omega r + h_c \tag{41}$$

where the mass and speed of sound are assumed to be constant. This parameterization is done as a check to ensure the consistency of the current work. The variables to be optimized include h_a, h_b, h_c, M_0, throttle on-r_u, and throttle off-r_d, to minimize the cost function given in Eq. (39). These results are shown in Table 4, with the results obtained by Chuang and Morimoto[9] given for comparison. All load factors are seen to be within acceptable limits. The periodic solution is compared with the steady-state solution, which only needs to optimize h and M. Table 4 also shows the steady-state results, again with Chuang and Morimoto for comparison, and shows the fuel savings of the periodic cruise trajectory. The steady-state trajectory resulted in a constant $\alpha = 5.36$ deg, $L/D = 4.18$, and a heating rate of 320 W/cm^2. As can be seen, both codes produce similar solutions with only a very slight difference. This minute discrepency may be because of the work of Chuang and Morimoto, who use a polynomial curve fit to the discontinuities in the standard atmosphere model, which may cause the optimizers to find different solutions; or the discrepency may be because of differences in the integration step size. This study used integration step sizes of 150 m, which resulted in accurate solutions without long CPU times.

Table 4 Results of Parameterization 1 optimization

Variable	Value	Chuang and Morimoto[9]	% Difference
h_a	8274 m	9551 m	13.37
h_b	−753 m	−810 m	7.04
h_c	45,284 m	45,942 m	1.43
r_f	1,194,041 m	1,194,041 m	0.0
M_0	14.815	14.694	0.82
r_u	604,993 m	603,606 m	0.23
r_d	851,032 m	835,062 m	1.91
J_p	0.001502 kg/m	0.001501 kg/m	0.07
h	42,600 m	42,376 m	0.53
M	14.419	14.37	0.34
J_{ss}	0.001556 kg/m	0.001555 kg/m	0.06
% fuel savings (J_p/J_{ss})	3.5	3.5	0.0

Parameterization 2

The second altitude parameterization allows the speed of sound to vary with altitude. The mass is still assumed to be constant and the altitude profile is still given by Eq. (41). The rest of the optimization is exactly the same as Parameterization 1. The steady-state results have constant $\alpha = 5.84$ deg, $L/D = 4.16$, and a heating rate = 301 W/cm^2. The fuel-consumption rate for the periodic case is 0.001564 kg/m, and the steady-state fuel consumption is 0.001666 kg/m. As can be seen, by allowing the speed of sound to vary with altitude, an increased fuel savings is obtained, corresponding approximately to a factor of two times greater than the constant speed-of-sound case.

Parameterization 3

In Parameterization 3, a changing mass because of fuel expenditure is added to the vehicle dynamics. Everything else is kept the same as Parameterization 2. Steady-state results gave an $\alpha = 5.84$, $L/D = 4.16$, and a heating rate of 301 W/cm^2 at the beginning of flight, and an $\alpha = 5.73$, $L/D = 4.17$, and a heating rate of 301 W/cm^2 at the end of the flight. The fuel-consumption rate for periodic cruise is 0.001545 kg/m, compared with the steady-state value of 0.001648 kg/m, for a 6.25% fuel savings. The change in mass produces a slight increase in fuel savings. An interesting result is that by allowing the mass to change, the steady-state solution decreases in value over Parameterization 2. This is reasonable because the vehicle becomes lighter and, therefore, less fuel is needed to maintain a level flight. This same reasoning also explains the difference in the periodic cost function.

Parameterization 4

In Parameterization 4, the range is allowed to vary to get an optimal r_f. Otherwise, the parameterization is the same as Parameterization 3. Steady-state results were similar to Parameterization 3. The fuel-consumption rate is 0.001543 kg/m for periodic cruise, and it is 0.001648 kg/m for steady-state cruise, producing a 6.37% fuel savings. As can be seen, the percentage of fuel savings is greatest in the parameterization that includes the largest number of variable parameters. The results for this parameterization are close to those of the constant mass solution. The fuel savings differ only by 1.88% in favor of Parameterization 4. It is important to include this effect in the numerical optimization along with allowing the mass to vary over the trajectory. The corresponding trajectory graphs are shown in Figs. 4–9 for Parameterizations 1–4.

Parameterization 5

Parameterization 5 draws upon the analysis presented for the mass-spring-damper system that was discussed earlier. An exponential decay term scales the harmonic portion of the altitude profile:

$$\exp[-\eta(r/r_f)](h_a \cos \omega r + h_b \cos 2\omega r) + h_c \qquad (42)$$

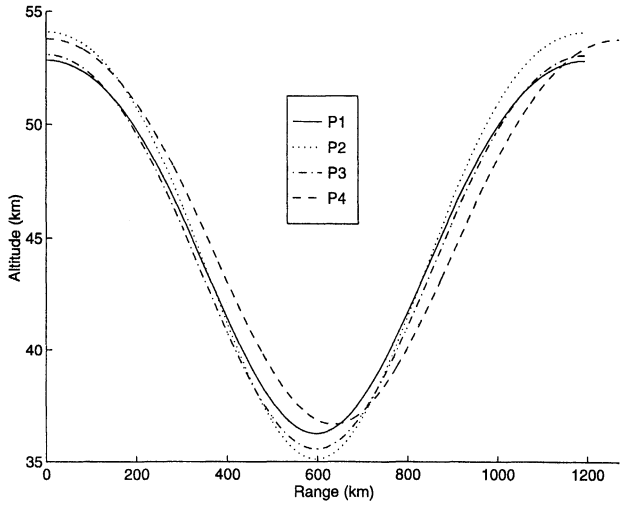

Fig. 4 Altitude vs range for Parameterizations 1–4.

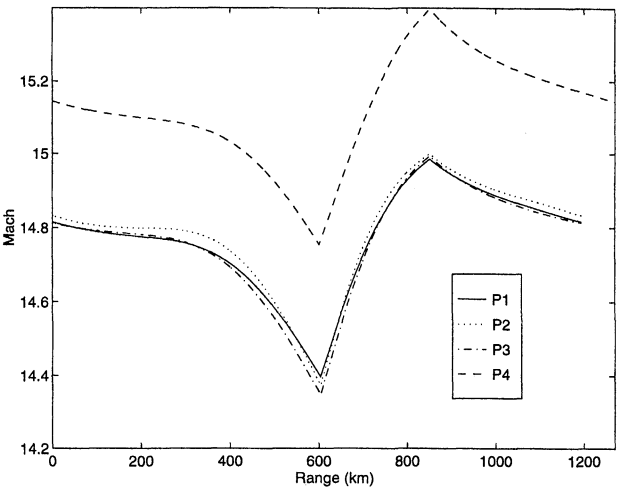

Fig. 5 Mach number vs range for Parameterizations 1–4.

This adds an extra degree of freedom, η, to the optimization. The constraint placed on the final Mach number is that the K.E./P.E. ratio be equal at the end and beginning of the period. The final height and flight-path angle are dictated by the altitude profile. Thus, three final state conditions are established at the end of the period, allowing the TPBVP to be fully specified. The results are shown in Figs. 10 and 11. Again, steady-state results were similar to Parameterizations 3 and 4. The fuel-consumption rates are 0.0009102 and 0.001648 kg/m for periodic and steady-state cruise, respectively. As can be observed, a fuel savings of 45% is possible using a damped pe-

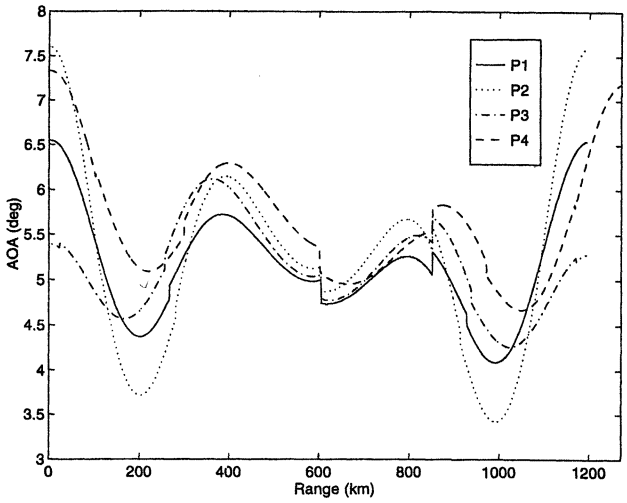

Fig. 6 Angle of attack vs range for Parameterizations 1–4.

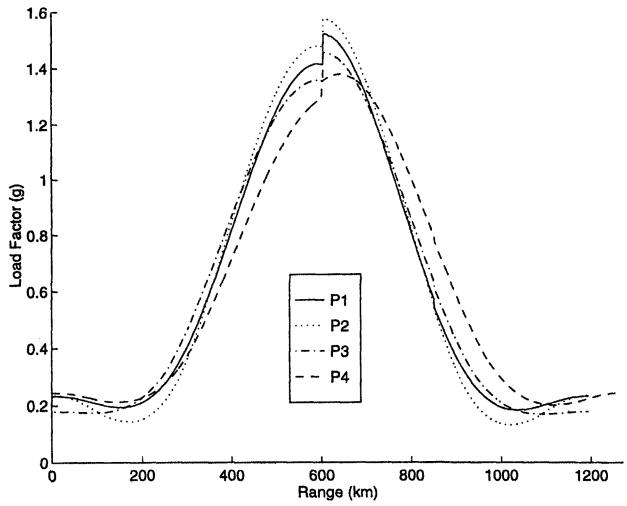

Fig. 7 Load factor vs range for Parameterizations 1–4.

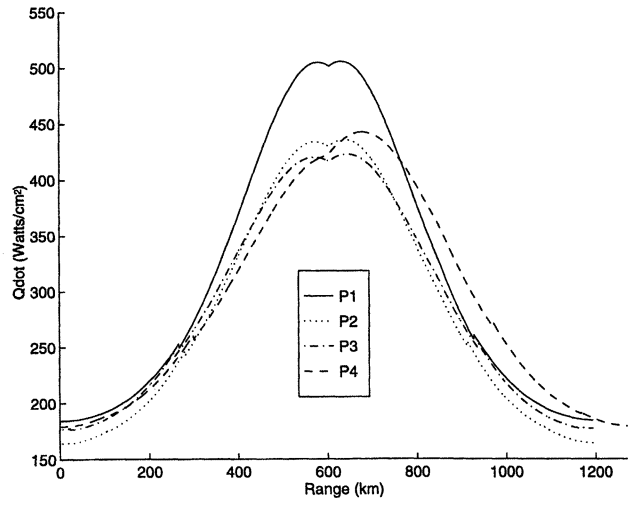

Fig. 8 Heating rate vs range for Parameterizations 1–4.

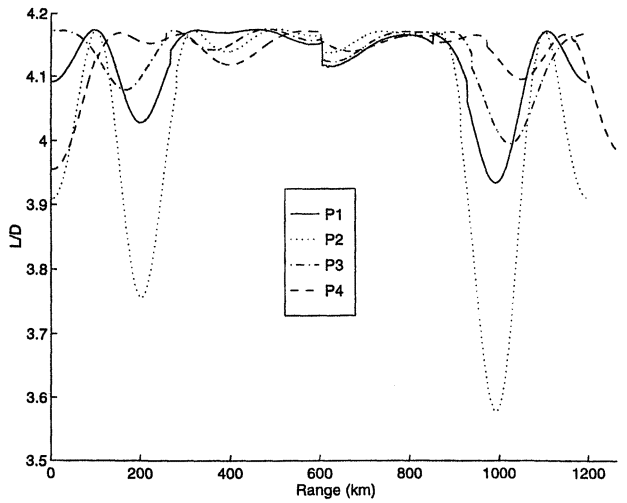

Fig. 9 *L/D* vs range for Parameterizations 1–4.

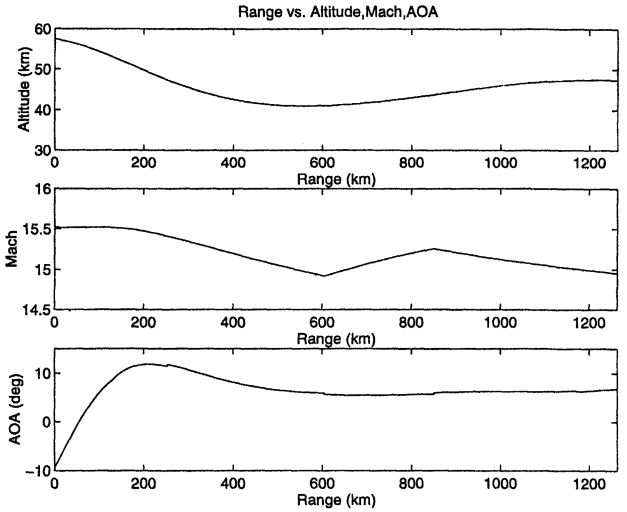

Fig. 10 Optimal periodic trajectory for Parameterization 5.

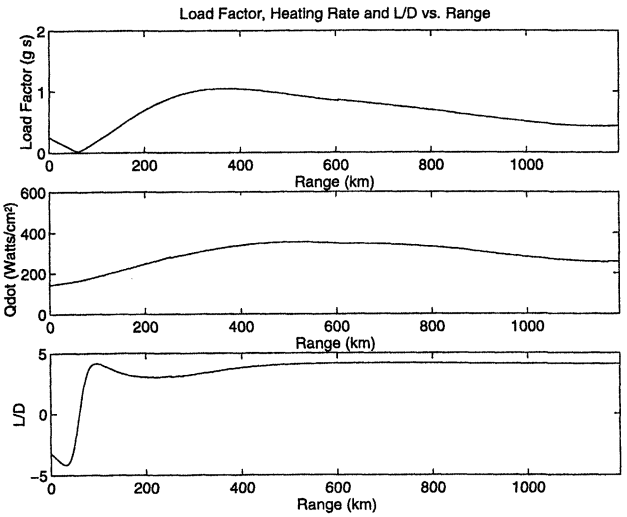

Fig. 11 Optimal periodic trajectory for Parameterizxation 5.

riodic cruise trajectory. This large fuel savings is achieved because the vehicle does not need to expend fuel to reach the initial height and Mach number. Figure 12 displays the effect of energy dissipation over one cycle for the various altitude parameterizations. The suboptimal damped solution attempts to find the path of least resistance with minimal fuel expenditure. As the range increases, these damped periodic trajectories will approach steady-state behavior.

A concern that arises from these damped trajectories is their effective fuel savings over multiple periods for long-range flight. Additional research is required to fully understand the maximum benefits of damped periodic cruise trajectories for

Table 5 Summary of parameterization results

Variable	Chuang and Morimoto[9]	P1	P2	P3	P4	P5
η	——	——	——	——	——	1.809
h_a, m	9551	8274	9470	8737	8537	11,256
h_b, m	−810	−753	−962	−625	−725	751
h_c, m	45,942	45,284	45,550	44,935	45,935	45,429
r_f, m	1,194,041	1,194,041	1,194,041	1,194,041	1,271,072	1,263,807
M_0	14.694	14.82	14.83	14.81	15.15	15.521
r_a, m	603,606	604,993	604,951	604,975	601,774	604,916
r_d, m	835,062	851,032	851,039	851,038	851,035	850,999
J_p, kg/m	0.001501	0.001502	0.001564	0.001545	0.001543	0.0009102
h, m	42,376	42,600	43,193	43,193	43,193	43,193
M	14.37	14.419	14.8	14.8	14.8	14.8
J_{ss}, kg/m	0.001555	0.001556	0.001666	0.001648	0.001648	0.001648
% fuel savings	3.5	3.5	6.12	6.25	6.37	44.77

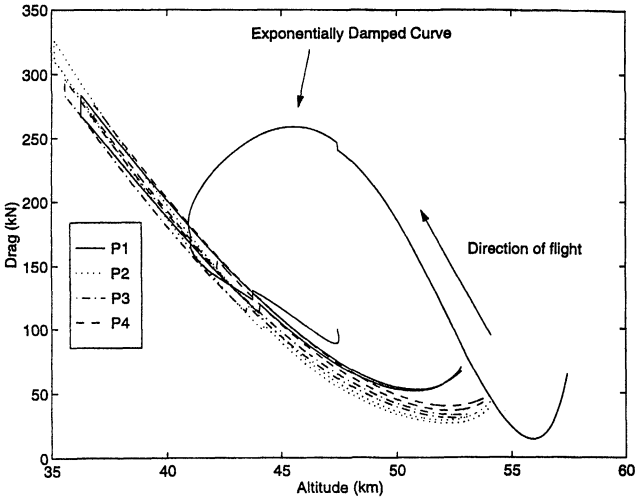

Fig. 12 Drag force vs altitude.

hypersonic flight. Purely periodic trajectories have the same fuel-consumption savings over each period. Fuel savings for damped trajectories are different over each cycle. In addition, damped solutions all eventually approach steady-state cruise flight. Because damped trajectories are not repetitive, the connections of damped solutions from one cycle to the next become important for long-range flight. It should be noted that the spring-mass-damper analogy assumes linear damping. It is obvious that the atmosphere is nonlinear and that the results given could be improved by applying nonlinear damping models. This could be done by developing an optimal solution instead of a suboptimal one for multiple periods.

A complete summary of the results for the altitude parameterizations can be seen in Table 5. This table shows that as the number of parameters in the altitude profile increases, better fuel savings are achieved. The drastic increase of damped trajectories clearly stands out and shows a promising new type of hypersonic periodic cruise.

Summary and Conclusions

An exponentially damped parameterized form of the altitude profile for periodic hypersonic flight has been introduced and shown to yield enhanced fuel-consumption savings over steady-state cruise. With this damped form of the parameterized altitude profile, solutions of the TPBVP are possible by imposing the constraint that the ratio of K.E./P.E. remain constant at the endpoints of a period. Optimization results indicate that the vehicle attempts to find the path of least resistance from an aerodynamic perspective while minimizing the fuel-consumption rate. Suboptimal solutions of the damped parameterized form of the altitude profile lead to fuel-consumption savings of approximately 45% over the initial period. This represents approximately an order of magnitude improvement over previous results. Without any loading constraints imposed on the optimization, heating rates and g loads are also found to be well within acceptable limits.

Even greater fuel-consumption rate savings may be possible if a nonparameterized form of the altitude profile is used in an unconstrained optimization. In addition, because the aerodynamic forces are actually nonlinear, it may be possible to develop a more accurate model of these forces to obtain better suboptimal trajectories for hypersonic flight. Such solutions will enhance efforts to achieve long-range flight.

Acknowledgments

The first author would like to thank the Department of Aerospace Engineering at the Unversity of Maryland, College Park, Maryland, for providing support for this research.

References

[1]Edelbaum, T., "Maximum Range Flight Paths," United Aircraft Corp., Rept. R-22465-24, 1955.

[2]Zagalsky, N. R., Jr., Irons, R. P., and Schultz, R. L., "Energy State Approximation and Minimum-Fuel Fixed Range Trajectories," *Journal of Aircraft*, Vol. 8, No. 6, 1971, pp. 488–490.

[3]Speyer, J. L., "On the Fuel Optimality of Cruise," *Journal of Aircraft*, Vol. 10, No. 12, 1973, pp. 763–765.

[4]Gilbert, E. G., "Vehicle Cruise: Improved Fuel Economy by Periodic Control," *Automatica*, Vol. 12, 1976, pp. 159–166.

[5]Speyer, J. L., "Nonoptimality of the Steady-State Cruise," *AIAA Journal*, Vol. 14, No. 11, 1976, pp. 1604–1610.

[6]Houlihan, S. C., Cliff, E. M., and Kelley, H. J., "Study of Chattering Cruise," *Journal of Aircraft*, Vol. 19, No. 2, 1982, pp. 119–124.

[7]Speyer, J. L., Dannemiller, D., and Walker, D., "Periodic Optimal Cruise of an Atmospheric Vehicle," *Journal of Guidance, Control, and Dynamics*, Vol. 8, No. 1, 1985, pp. 31–38.

[8]Chuang, C.-H., and Speyer, J. L., "Periodic Optimal Hypersonic Scramjet Cruise," *Optimal Control Applications and Methods*, Vol. 8, 1987, pp. 231–242.

[9]Chuang, C.-H., and Morimoto, H., "Periodic Optimal Cruise for a Hypersonic Vehicle with Constraints," *Journal of Spacecraft and Rockets*, Vol. 34, No. 2, 1997, pp. 165–171.

[10]Engineering, V., *Dot User Manual, Version 4.00*, 1st ed., Vanderplaats, Miura, and Associates, Goleta, CA, 1993.

[11]Schultz, R. L., and Zagalsky, N. R., "Aircraft Performance Optimization," *Journal of Aircraft*, Vol. 9, No. 2, 1972, pp. 108–114.

[12]Schultz, R. L., "Fuel Optimality of Cruise," *Journal of Aircraft*, Vol. 11, No. 9, 1974, pp. 586, 587.

[13]Gilbert, E. G., and Parsons, M. G., "Periodic Control and the Optimality of Aircraft Cruise," *Journal of Aircraft*, Vol. 13, No. 10, 1976, pp. 828–830.

[14]Grimm, W., Well, K. H., and Oberle, H. J., "Periodic Control for Minimum-Fuel Aircraft Trajectories," *Journal of Guidance, Control, and Dynamics*, Vol. 9, No. 2, 1986, pp. 169–174.

[15]Sachs, G., and Christodoulou, T., "Reducing Fuel Consumption of Subsonic Aircraft by Optimal Cyclic Cruise," *Journal of Aircraft*, Vol. 24, No. 9, 1987, pp. 616–622.

[16]Speyer, J. L., "Periodic Optimal Flight," *Journal of Guidance, Control, and Dynamics*, Vol. 19, No. 4, 1996, pp. 745–753.